THE CURRENT STATUS OF CLOUD TOP HEIGHT REMOTE SENSING FROM SEVIRI: UPDATED ASSESSMENT INCLUDING TWO NEW ALGORITHMS

Ulrich Hamann[1,2], Andi Walther[3], Stephan Kox[4], Ayako Takeuchi[5], Ralf Bennartz[3], Jan Fokke Meirink[1], Bryan Baum[3], Rob Roebeling[4]

[1]KNMI, De Bilt, Netherlands
[2]now at MeteoSwiss, Locarno, Switzerland
[3]University of Wisconsin-Madison, Madison, Wisconsin, USA
[4]EUMETSAT, Darmstadt, Germany
[5]Meteorological Satellite Center, Japan Meteorological Agency, Tokyo, Japan

Abstract

The International Clouds Working Group (ICWG) investigates strengths and weaknesses of state-of-the-art cloud retrievals from passive and active sensors. Therefore, a common retrieval data base was established. Hamann et al. (2014) inter-compared eleven state-of-art cloud top height SEVIRI datasets and validated them against CALIOP and CPR measurements. Recently, algorithms of the Japan Meteorological Agency (JMA) and of the German Aerospace Center (DLR) joined the evaluation project. The JMA algorithm is based on EUMETSAT's Nowcasting-SAF software package. The DLR algorithm named COCS is designed to derive the properties of high ice clouds. It is the first neural network retrieval investigated in this framework. In this extended abstract, we discuss the performance of the two new retrieval algorithms in comparison to the others.

1. INTRODUCTION

Covering about 70% of the earth's surface clouds strongly influence solar and thermal radiative transfer and the earth's water cycle. According to Boucher et al. (2013), their direct and indirect climate effects as well as feedback mechanisms remains the largest uncertainty in climate radiative forcing. Hazardous weather situations as strong precipitation and wind gusts are primarily caused by convective activity inside clouds. Therefore, there is an urgent need for accurate cloud observations in order to monitor climate change and validate climate models. Passive satellite imagers measuring radiation at visible to thermal infra-red wavelengths provide a wealth of information on cloud properties. To understand the uncertainty characteristics of the retrievals an in depth analysis and validation of the retrieval data sets is required.

In 2014 the International Clouds Working Group (ICWG) within the Coordination Group for Meteorological Satellites (CGMS) was endorsed. This working group aims to assess the current status of cloud remote sensing from passive imagers from different providers. Integral part of the working group activities are the so called Cloud Retrieval Evaluation Workshops (CREW) that provide a forum for exchange and collaboration were organised (Roebeling et al., 2012). Exchange during the workshops, which have been organised since 2006, triggered the creation of a common cloud retrieval database enabling a systematic inter-comparison and evaluation of the most recent retrieval datasets. In this extended abstract we present the inter-comparison and validation results of the SEVIRI cloud top height (CTH) algorithms with special focus on the datasets of the Japan Meteorological Agency and COCS algorithm of the DLR that recently joined the ICWG retrieval inter-comparison.

2. DATASETS

During the CREWs a common retrieval database was created containing cloud remote sensing data from SEVIRI, AVHRR, MODIS, MISR, AIRS and POLDER (Roebeling et al., 2012; Hamann et al., 2014). As reference sensors CPR, CALIOP and AMSR-E are included, DARDAR is scheduled for implementation. The cloud properties stored in the CREW database are cloud mask, cloud phase, cloud top temperature/pressure/height, cloud optical depth, effective radius, and cloud water path. The CREW database contains five days of data: the 13^{th} ,17^{th}, 18^{th}, 23^{rd} of June 2008 and the 3^{rd} of July 2008. Leading institutions with state-of-the-art SEVIRI cloud retrieval algorithms provided data to the CREW database: Climate Monitoring SAF (CMS), EUMETSAT (three algorithms EUM, OCA, MPF), Free University of Berlin (FUB), German Aerospace Center (two algorithms DLR and COX), MeteoFrance (MFR), Algorithm Working Group of University of Wisconsin-Madison (AWG), UK-MetOffice (UKM), NASA Goddard Space Flight Center (GSF), NASA Langley Research Center (LAR), Royal Meteorological Institute Belgium (RMB), and Japan Meteorological Agency (JMA)

3. ALGORITHM DESCRIPTION

The remote sensing algorithms investigated in this extended abstract use observation of the Spinning Enhanced Visible and InfraRed Imager (SEVIRI) onboard Meteosat Second Generation (MSG). The instrument is described in detail by Schmetz et al. (2002). SEVIRI has eleven spectral bands with 3 km spatial resolution at the sub-satellite point and one high-resolution broadband visible (HRV) channel at 1 km spatial resolution. The SEVIRI sensor scans the observation disk every 15 min. In the second part of the paper the SEVIRI retrievals are compared to measurements of CALIOP and CPR. The Cloud–Aerosol LIdar with Orthogonal Polarization (CALIOP) onboard CALIPSO is a dual wavelength lidar (532 and 1064 nm). The primary products are profiles of total backscatter, from which further products like cloud and aerosol properties are derived (Winker et al., 2003). On the Earth's surface individual CALIOP beams have a width of about 70 m with a sampling distance of 333 m. The vertical resolution of the CALIOP products is 30 to 60 m. The Cloud Profiling Radar (CPR) onboard CloudSat is a 94 GHz nadir-looking radar (Stephens et al., 2002). It measures the backscattered signal as a function of distance from the radar. CPR provides cloud and precipitation information with 500 m vertical resolution between the surface and 30 km. Its horizontal resolution is 1.4 km (cross-track) by 1.7 km (along-track).

Most of the SEVIRI remote sensing algorithms use the methods of radiance fitting, radiance ratioing, optimal estimation or a combination of those. A detailed description is given in Hamann et al. (2014). Hence, we describe only the algorithm of the Japan Meteorological Agency (JMA) and the COCS (COX) algorithm of the German Aerospace Center in detail.

The algorithm of the Japan Meteorological Agency is based on the methods developed by the EUMETSAT Nowcasting SAF (Meteo-France, 2012). It involves threshold techniques using brightness temperatures and reflectivities for cloud mask and cloud type/phase retrieval. Threshold selection for cloud mask tests is based on the algorithm developed by NOAA/NESDIS for GOES-R product (Heidinger, 2011b). Radiance fitting, radiance ratioing and intercept method are applied for CTH assignment (Derrien, 2013). The algorithm uses radiative transfer calculation results obtained from the latest numerical prediction data to determine thresholds for clear sky radiance from infrared channels. The local radiative center (Heidinger, 2011a) is used in the JMA algorithm. A prototype product was produced using SEVIRI data. It was evaluated by comparing with MODIS products for two-week periods at every season in 2012. Cloud mask detection accuracy was 85 % and most of the other scores were also reasonable (Imai et al., 2014). However, the evaluation results also suggest the need for further improvement in cloud detection over snow/ice area and cloud height of semi-transparent cloud.

The COCS (Cirrus Optical properties derived from CALIOP and SEVIRI during day and night) algorithm retrieves CTH and cloud optical depth (COD) of cirrus clouds from SEVIRI measurements (Kox et al., 2010, 2012, 2014). The COCS algorithm (COX) is an artificial neural network (ANN) with one input, one hidden, and one output layer. It uses the brightness temperatures of four infrared channels (7.3, 9.7, 8.7, and 13.4 µm) and three brightness temperature differences (6.2 – 7.3, 8.7 – 12.0 µm, 10.8 – 12.0 µm) of SEVIRI as well as some auxiliary datasets (latitude, viewing zenith angle, and land-sea-mask) as input; hence, it has 10 neurons in the input layer. According to the complexity of the retrieval problem and the size of the training dataset, the hidden layer was designed with 600 neurons. The ANN is trained with 8,000,000 and validated with another 1,000,000 co-incident and quasi simultaneous observations of CALIOP and SEVIRI (July 2006 – June 2009) using the COD and CTH derived from the 5 km cloud layer product of CALIOP. Kox et al. (2014) describe a procedure for the quality control of the training and validation dataset. First, since the LIDAR signal of CALIOP becomes saturated with increasing optical depth, the CALIOP COD was limited to a maximum of 2.5. Greater values were reported as opaque cloud. As a result, the focus of COX is on thin cirrus clouds. Second, clouds with a cloud mid layer temperature above 243 K are excluded. And third, to exclude aerosol layers misclassified as cirrus clouds, a latitude dependent CTH minimum $z_{top,\ min}$ was chosen. $z_{top,\ min}$ is 4.5 km at high latitudes and increases to 9.5 km at 22°N or 22°S respectively. For latitudes smaller than 22° the minimum CTH is kept constant at 9.5 km. The COX retrieval was verified against CALIOP measurements and validated against airborne HSRL lidar measurements during the WALES and PAZI measurement campaign (Kox et al., 2012, 2014). The validation shows an excellent performance of the algorithm with a detection efficiency of over 99% and a false alarm rate small than 5% for clouds with COD > 0.1. Kox et al. (2010) remark, that the spatial variation of the COD derived by COX is less than the one derived by CALIOP. They explain this behaviour with the different spatial resolution of the two sensors. Kox et al. (2010) also mention some difficulties in retrieving the COD for latitudes larger than 60º. COX is the first neural network method in the CREW dataset; hence, the comparison with the other SEVIRI retrieval datasets has the potential to reveal strengths and weaknesses of applied retrieval methods.

4. INTER-COMPARISON OF CLOUD TOP HEIGHT AND PHASE

In the following analysis we concentrate on the algorithms providing both CTH and CPH. In Figure 1 the CPH is shown for the 13th of June 2008, 13:45UTC. There is a good agreement between the different algorithms. Ice clouds are mainly detected in the ITCZ and within the frontal systems in the mid-latitudes. Water clouds are primarily detected above the Atlantic and Indian Ocean. Some deviation between the algorithms can be identified, in particular at the edge of cloudy areas in the tropics and along the frontal systems in the mid–latitudes. LAR observe the highest fraction of water clouds (35 %). COX and JMA observe the highest fraction of ice clouds in comparison to the other algorithms. MFR, AWG, and JMA decided to introduce an unknown cloud phase category. MFR shows unknown cloud phase all over the disk, especially over the Atlantic Ocean. AWG shows some cases of undetermined clouds in the northern and southernmost part of the disk. Areas with no retrievals include cloud free regions as well as cases that are discarded due to retrieval challenges. CMS, UKM and GSF make use of solar channels for the cloud phase determination. No cloud retrievals are conducted in the south-eastern part of the observed disk for this specific position of the Sun; hence, the fraction of observations with no retrievals is 54 % or above for these retrievals. CMS neither performs cloud detection for the Sun glint area, perceivable as semicircle of no data close to Sierra Leone for the given time. MFR, JMA, and LAR have the lowest no data fraction of about 42 %.

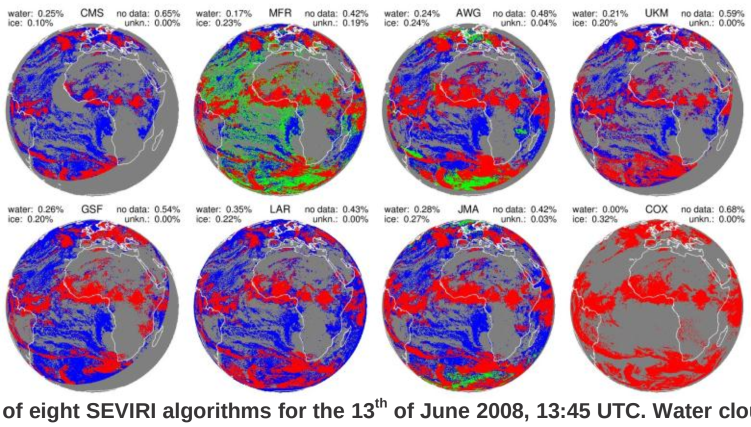

Figure 1: **Cloud phase of eight SEVIRI algorithms for the 13th of June 2008, 13:45 UTC. Water clouds are shown in blue, ice clouds in red, and clouds with an unknown phase in green. The lower right picture shows the result of the neural network retrieval COX that is designed for the retrieval of cirrus cloud properties only.**

In Figure 2 the retrieved CTH datasets are inter-compared. Fig. 2 A show the CTH of all clouds. The CTH retrieval comparison for all clouds is similar to the analogous inter-comparison of the CTP in Hamann et al. (2014). In Fig. 2 B the CTH is shown only for clouds identified as ice clouds by the individual retrieval. Additionally, COX is shown here. Note the effect of the limited area of the cloud phase detection of CMS, UKM, and GSF due to the discarded regions of high solar zenith angles and Sun glint. The CMS classifies only 10 % of the pixels as covered with ice clouds, whereas COX does so for 32 %. Most of the algorithms but UKM and COX retrieve a mean ice CTH of around 10 km for this particular scene. The UKM algorithm retrieving a mean ice CTH of 7.8 km classifies many pixels over the South Atlantic as ice clouds with a very low CTH, that are not classified as ice clouds by all other algorithms. Furthermore, UKM has a restrictive ice cloud mask in the tropics; hence, the high clouds in these regions contribute less to the mean ice CTH. COX derives larger CTH values than any other algorithm in every region of the disk resulting in a mean ice CTH of 12.4 km.

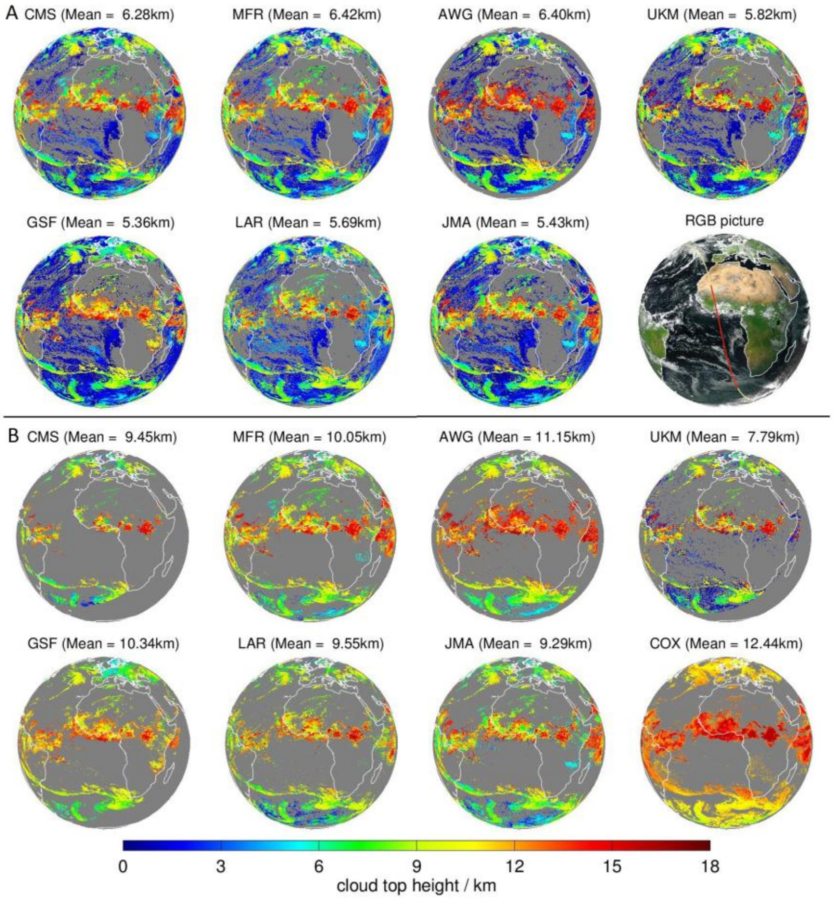

Figure 2: **Cloud top height retrievals inter-comparison for the 13th of June 2008, 13:45 UTC. The first two rows show the CTH retrieval for all cloud phases. The last figure in the second row shows the false colour image of this SEVIRI scene. In yellow the path of the ATRAIN satellite constellation is shown. The part of the ATRAIN path between 13:45 UTC and 14:00 UTC is marked in red. The third and fourth row show the CTH only for ice clouds.**

5. COMPARISON OF THE CLOUD TOP HEIGHT TO CALIOP AND CPR

To quantify the accuracy of the SEVIRI CTP/CTH retrievals, the SEVIRI data sets are validated against CALIOP and CPR retrievals. CALIOP and CPR are part of the A-train satellite constellation traveling over the SEVIRI disk. The left hand side of Figure 3 shows a false colour images of the SEVIRI disk. The false colour image depicts that the path of the A-train satellite constellation flies above deep convective system located above the Ivory Coast. The right hand site of Figure 3 illustrates the comparison of the SEVIRI with the CALIOP and CPR retrievals. The panels show the CALIOP backscatter and CPR reflectivity signal. The CTHs detected by CALIOP and CPR are marked in green and red, respectively. CALIOP detects a cloud layer at about 16 km between 0°N and 15°N. The LIDAR beam does not penetrate further into the cloud then an optical depth of 3 to 5; therefore, the CALIOP backscatter is limited to the upper part of optically thick clouds. In contrast, CPR is not as sensitive to low extinctions, but penetrates deeper into optically thick clouds; hence, the CTH detected by CPR is lower than the one of CALIOP. The CPR reflectivity indicates the high optical depth of the deep convective system over the Ivory coast at 6.5°N to 8.5°N. Between 2.0°N and 5.5°N two cloud layers - one at 10 to 14 km height and one at 1 to 5 km height - can be identified with the CPR reflectivity.

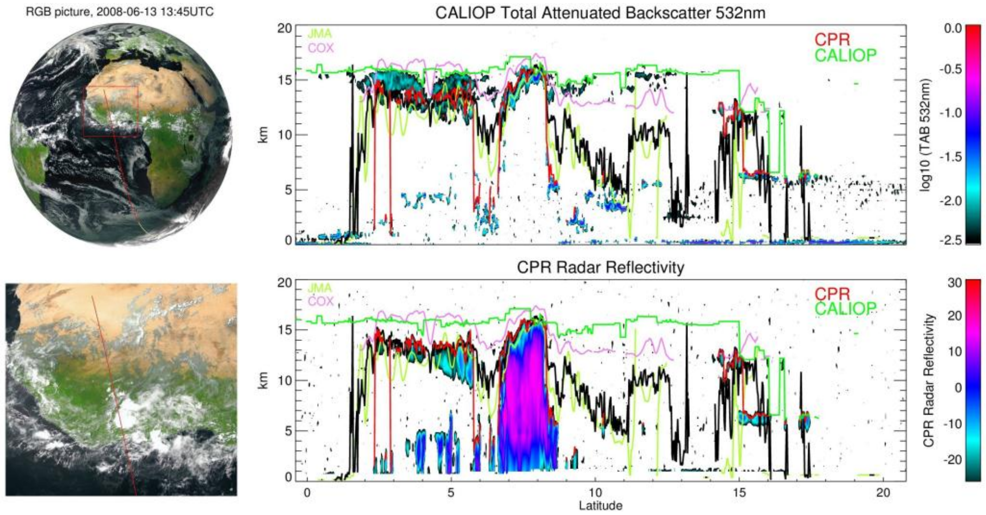

Figure 3: **Illustration of the validation method of the SEVIRI cloud top height (CTH) retrievals with CALIOP and CPR for the 13th of June 2008, 13:45 UTC. In the top left panel the overflight path of the A-train is marked in yellow, the part of the path that the A-train travels within 15 min is marked in red. The lower left image shows the region that is investigated in more detail on the right hand side. In the panels on the right the CALIOP backscatter and the CPR reflectivity illustrate the vertical structure of the clouds and the CTH derived from these instruments. Additionally the CTHs derived by COX and JMA are shown. The black line represents the mean of all SEVIRI CTH algorithms.**

Additionally the CTHs of JMA and COX as well as the mean of all SEVIRI algorithms are shown. At the core of the deep convective system, the upper cloud boundary is usually sharp and the extinction coefficient is high; hence, the agreement of the SEVIRI algorithms as well as CALIOP and CPR is very good. In the multi-layer region, most of the SEVIRI retrievals tend to follow the CPR CTH rather than the CALIOP CTH. Between 9°N and 15°N CALIOP detects an optically thin cloud layer which is not detected by the CPR. A few clouds between 1 and 5 km can be identified in the CALIOP backscatter signal. The SEVIRI algorithms retrieve quite different CTHs for this region. The situation of a thin cirrus cloud over another cloud is a challenging condition for passive CTH retrievals. All algorithms retrieve CTHs largely lower than the CALIOP CTH. An exception is COX being closer to the CALIOP than to the CPR CTH. The COX CTH is observed to be larger than CALIOP in the region of multi-layer clouds and the deep convective system where the upper cloud layer has a sufficiently high optical depth. Between 8.3°N to 12.6°N the COX CTHs are lower than those of CALIOP, but still high compared to the results of the other algorithms.

Figure 4 shows scatter plots for the comparison of the SEVIRI algorithms to CALIOP and CPR. The statistics include three overpasses of the A-train satellite constellation 11317 to 11319. The comparison is realized for a common mask, which means that all SEVIRI algorithms as well as the reference instrument are able to retrieve a CTH for the pixels taken into account. In comparison to CALIOP, see Fig. 4 A, the majority of the scatter points are on the lower right side of the one-to-one line for all algorithms expect COX, meaning that the SEVIRI CTHs are lower than those of CALIOP. The bias SEVIRI minus CALIOP CTH is negative for all SEVIRI retrievals ranging from -2.8 km (MPF) to -1.0km (AWG), except for COX (+3.0 km). Clouds with a CALIOP CTH at about 15 km are associated with the TTL. The CTH of these clouds are nicely captured by AWG, GSF, and COX. The other algorithms also retrieve a maximum cloud occurrence at about 12km, but show some more cases of underestimation for these clouds. Fig. 4 B shows the same comparison, but against CPR. In contrast to the comparison to CALIOP, SEVIRI CTH are about in the same height as CPR. OCA, AWG, UKM, GSF, and COX tend to detect CTHs higher than the CPR. Apart from COX the SEVIRI minus CPR CTH biases range from -0.8 km (DLR) to 0.8 km (AWG). For CTHs above 10 km COX corresponds very well to CALIOP and is slightly higher than the CPR CTH. But for CTHs lower than 10 km retrieved by CALIOP and CPR, COX shows an unusual behaviour. COX retrieves CTHs between 10 and 12 km more or less unrelated to the CALIOP and CPR CTH, clearly more pronounced than the occasional cases of overestimation of the other algorithms.

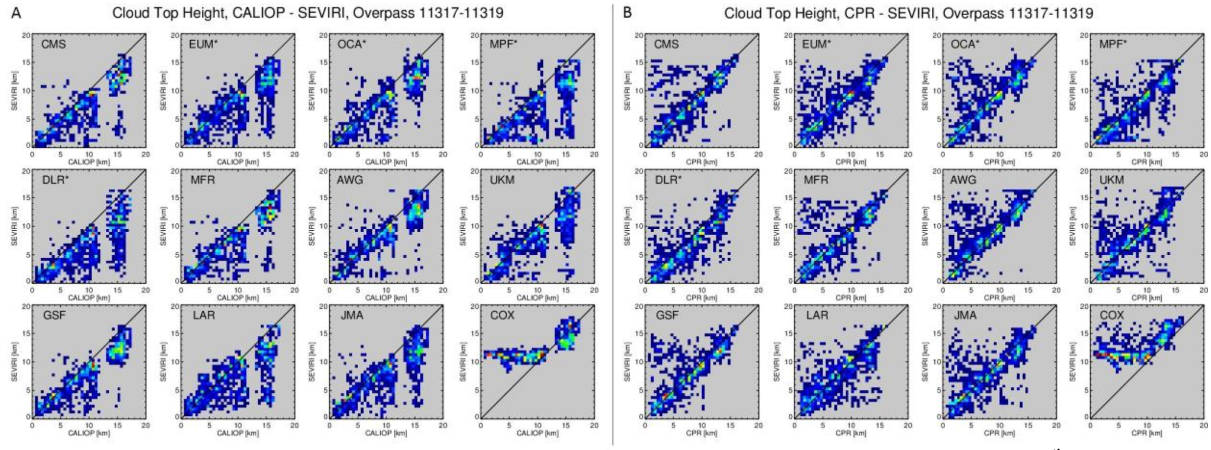

Figure 4: **Scatter plots of the cloud top height SEVIRI data sets against CALIOP (A) and CPR (B) for 13th of June 2008, 12:00–15:30 UTC (A-train overpasses 11317–11319). In case a SEVIRI algorithm only provides CTP and not the CTH, CTP values were transformed to CTH values using temperature profiles as provided in the ECMWF-AUX product of the CloudSat data processing centre. In this case the algorithm acronym is marked with a star.**

6. TAYLOR DIAGRAMS COMPARISON TO CALIOP AND CPR

The Taylor diagram offers a way to illustrate an ensemble of datasets in a very compact form. It uses the standard deviation of the investigated dataset normalized by the standard deviation of the reference dataset as radial coordinate and the arc cosine of the correlation coefficient as polar coordinate. The point with a normalized standard deviation of one and a correlation of one represents an ideal agreement. The distance between this point and the marker of the investigated dataset is equal to the centred pattern root mean square difference E’ (Taylor, 2001).

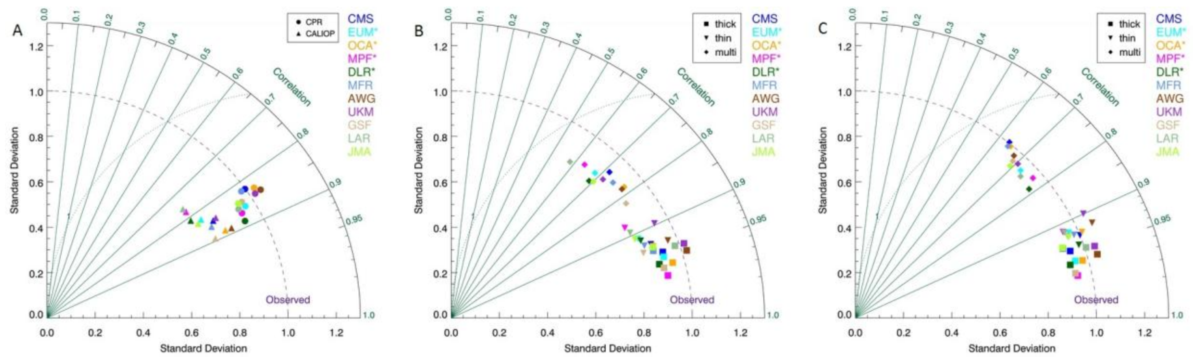

Figure 5: **Taylor diagram comparing the SEVIRI data sets with CALIOP and CPR for 13th of June 2008, 12:00–15:30 UTC (A-train overpasses 11317–11319). The Taylor diagram shows the standard deviation of the SEVIRI retrieval divided by those of the reference sensor as radial coordinate and the arc cosine of the correlation coefficients of these data sets as angle. Figure A shows the comparison against CALIOP (circles) and CPR (triangles). Figure B shows the comparison against CALIOP for three cloud categories: optically thick and thin single layer clouds and multi-layer clouds. Figure C is the same as B, but with CPR as reference instrument.**

Figure 5 A shows the Taylor diagrams for the comparison of the SEVIRI retrievals with CALIOP and CPR observations. The correlation of the SEVIRI datasets and the reference datasets is between 0.75 and 0.90. The standard deviations of the SEVIRI data sets are comparable to the CPR, but smaller than that of CALIOP. Using the centred pattern root mean square difference E’ as the quality measurement, we find that the ranking of the algorithms depends on the reference dataset. E.g., the DLR algorithm has the lowest (best) E’ with respect to the CPR, but a large E’ with respect to CALIOP in comparison to the other SEVIRI datasets. Figure 5 B and C are similar to Figure 5 A, but the results are shown for three cloud categories: Optically thin and thick single layer clouds as well as multi-layer clouds. The CALIOP product “number of layer” is used to distinguish single and multi-layer clouds. Single layer clouds are classified as optically thin clouds, if their CALIOP cloud optical depth is smaller than 3, otherwise as optically thick. The best agreement is found for optically thick clouds. The correlation coefficients are above 0.95 and the normalized standard deviation is about one. For thin single layer clouds the correlation coefficients are between 0.90 and 0.95. For multi-layer clouds the correlation coefficients are between 0.58 and 0.82.

7. DISCUSSION

The deviation between COX and the other algorithms can be attributed to a major part to the different retrieval methods. Apart from COX all algorithms use radiance fitting, radiance ratioing (CO_2 slicing), optimal estimation or a combination of those (Hamann et al., 2014). The retrieved CTH is a radiatively effective one and represents a level of an optical depth of one measured from the cloud top. In contrast, CALIOP is sensitive to very small extinction coefficients. Hence, the CTH retrieved by CALIOP is known to be on average 1 to 2 km higher as the effective CTH (e.g. Minnis et al., 2008). If the extinction coefficient is very low, the difference of the radiatively effective and CALIOP CTH can be several km. COX is based on an artificial neural network (ANN) using CALIOP as training dataset. Hence, it is expected that COX rather reproduce the CALIOP CTH than a radiatively effective CTH. Therefore, COX CTHs are expected to be higher than those of the other SEVIRI retrievals.
As the ANN of COX aims to reproduce CALIOP CTHs, it is plausible that COX CTHs are occasionally higher than CALIOP CTHs. Ideally, the remaining residual should be as small as possible. However for clouds lower than 10 km COX reports CTHs between 10 and 12 km. This behaviour could be caused by different reasons: One reason is the utilization of a former version (v 2.x) of the CALIOP level 2 datasets resulting in a reproduction of different artificial features within the CALIOP results by COX; hence, too many clouds are detected, in particular over sea surfaces. Another reason is possibly the specific training method of the ANN. Kox et al. (2014) introduced filters to ensure that the training dataset for the ANN includes ice clouds only as described in section 3. These filters might have excluded cases of low clouds too generously, which are relevant for the training the ANN for these cloud types. In particular, the latitude dependent prescribed minimum of the CTH is potentially a rigorous criterion. Still the COX dataset reproduces CTH very well for CALIOP CTH above 10 km. Not a single case of severe CTH underestimation was observed for COX at this height level. GSF, AWG, MFR, CMS and OCA retrieved also good results with only a few cases of CTH underestimations. For future studies it is suggested to investigate the behaviour of cloud detection and CTH retrieval by COX as function of latitude and/or cloud optical depth, e.g. comparing only clouds with COD > 0.2. For the discussion of the Taylor diagrams have a look at Hamann et al. (2014).

8. SUMMARY

Within the framework of the International Cloud Working Group (ICWG) a remote sensing database of the most recent passive and active cloud remote sensing algorithm was created. The CPH and CTH were inter-compared and validated against CALIOP and CPR measurements highlighting in particular the two newest algorithms joining this investigation: the algorithm of the Japan Meteorological Agency (JMA) and the artificial neural network retrieval COCS (COX) from the German Aerospace Center. A good agreement of the CTH was found. Some deviations were observed, in particular for the edges of the cloudy areas in the inter-tropical convergence zone (ITCZ). The basic distribution of water and ice clouds were similarly retrieved by all algorithms detecting mainly ice clouds in the ITCZ and within the frontal systems in the mid-latitudes, whereas water clouds were mainly detected over the Atlantic ocean. However, some substantial differences in the occurrence frequency of ice clouds could be observed ranging from 10% to 32% of all pixels. JMA and LAR had the smallest fraction of missing data for the cloud phase retrieval. In contrast, retrievals using solar observation suffered from the limited availability of these observations. These differences were partly attributed to different cloud phase determinations and partly due to exclusion of areas with challenging retrieval conditions. The mean CTH of ice clouds was found to be around 10 km for all algorithms except UKM and COX for a specific time slot. UKM retrieved a mean ice CTH of 7.8 km due to many very low ice in the South Atlantic, whereas COX retrieved a mean ice CTH of 12.4 km. The difference of COX to the other retrieval algorithms is probably due to two reasons. First, the neural network of COX was trained to reproduce the CALIOP CTH, which is in general above the radiatively effective CTH retrieved by the other algorithms. Second, for clouds with a CALIOP CTH below 10 km, the results of the COX algorithm seem to be affected by the limitation of the training dataset of the neural network. For further information about the International Cloud Working Group (ICWG) and the Cloud Retrieval Evaluation Workshops (CREW), please have a look at the project website: http://www.icare.univ-lille1.fr/crew.

ACKNOWLEDGEMENT

We would like to thank EUMETSAT for funding of the CLOUDSTATE fellowship as well as the CREW project including the Cloud Retrieval Evaluation Workshops in 2006, 2009, 2011, and 2014. We thank all institutions providing cloud retrieval datasets. We thank the ICARE Data and Services Center for providing access to the data used in this study and for hosting the project website of the International Cloud Working Group (ICWG). We thank Frank Fell and EUMETSAT for providing the AVAC-S software that was used extensively for this research. The views, opinions, and findings contained in this report are those of the author(s) and should not be construed as an official National Oceanic and Atmospheric Administration or US Government position, policy or decision.

REFERENCES

Boucher, O. and Randall, D. (2013): Chapter 7, Clouds and Aerosols, IPCC: climate change: the physical science basis. Contribution of working group I to the fifth assessment report of the inter-governmental panel on climate change

Derrien, M. and Le Gléau, H. (2013): Algorithm Theoretical Basis Document for "Cloud Products" (CMa-PGE01 v3.2, CT-PGE02 v2.2 & CTTH-PGE03 v2.2), NWCSAF, http://www.nwcsaf.org

Hamann, U., Walther, A., Baum, B., Bennartz, R., Bugliaro, L., Derrien, M., Francis, P., Heidinger, A., Joro, S., Kniffka, A., Le Gléau, H., Lockhoff, M., Lutz, H.-J., Meirink, J. F., Minnis, P., Palikonda, R., Roebeling, R., Thoss, A., Platnick, S., Watts, P., and Wind, G. (2014): *Remote sensing of cloud top pressure/height from SEVIRI: analysis of ten current retrieval algorithms*. Atmos. Meas. Tech., 7, 2839-2867, www.atmos-meas-tech.net/7/2839/2014/

Heidinger, A. K. (2011a). Algorithm theoretical basis document ABI cloud height. NOAA NESDIS Center for Satellite Applications and Research, *http://www.goes-r.gov/products/baseline-cloud-top-height-cloud-layer.html*

Heidinger, A. (2011b): Algorithm theoretical basis document ABI Cloud Mask. NOAA NESDIS CENTER for Satellite Applications and Research, http://www.goes-r.gov/products/baseline-clear-sky-mask.html

Imai, T., T. Izumi, K. Mouri, A. Takeuchi, K. Saito, and K. Shimoji (2014): Evaluation of cloud products for Himawari-8/-9, Presentation at the fourth Cloud Retrieval Evaluation Workshop 2014 (CREW-4)

Kox, S. H. Mannstein, F. Ewald, and B. Mayer, (2010): COCS - Cirrus Optical properties derived from CALIOP and SEVIRI during day and night time. EUMETSAT Conf. 2010 Proceedings, EUMETSAT.

Kox, S. (2012): Remote sensing of the diurnal cycle of optically thin cirrus clouds. PhD thesis, LMU Munich, Faculty of Physics.

Kox, S., L. Bugliaro, and A. Ostler (2014): Retrieval of cirrus cloud optical thickness and top altitude from geostationary remote sensing, Atmos. Meas. Tech., 7, 3233-3246, 2014, www.atmos-meas-tech.net/7/3233/2014/, doi:10.5194/amt-7-3233-2014

Minnis, P., C. R. Yost, S. Sun-Mack, and Y Chen (2008): Estimating the top altitude of optically thick ice clouds from thermal infrared satellite observations using CALIPSO data. Geophys. Res. Lett., 35, L12801, doi:10.1029/2008GL033947.

Roebeling, R., B. Baum, R. Bennartz, U. Hamann, A. Heidinger, A. Thoss, and A. Walther (2012): Evaluating and Improving Cloud Parameter Retrievals. Bulletin of the American Meteorological Society, **94**, ES41–ES44, http://journals.ametsoc.org/doi/full/10.1175/BAMS-D-12-00041.1

Schmetz, J., P. Pili, S. Tjemkes, D. Just, J. Kerkmann, S. Rota, A. and Ratier (2002): An introduction to Meteosat second generation (MSG). B. Am. Meteorol. Soc., 83, 977–992.

Stephens, G. L., D. G. Vane, R. J. Boain, G. G. Mace, K. Sassen, Z. Wang, A. J. Illingworth, E. J. O'Connor, W. B. Rossow, S. L. Durden, S. D. Miller, R. T. Austin, A. Benedetti, C. Mitrescu, and The CloudSat Science Team (2002): The CloudSat mission and the A-Train: a new dimension of space-based observations of clouds and precipitation. B. Am. Meteorol. Soc., 83, 1771–1790.

Taylor, K. E. (2001): Summarizing multiple aspects of model performance in a single diagram, J. Geophys. Res.-Atmos., 106, 7183–7192.

Winker, D. M., J. Pelon, and M. P.McCormick (2003): The CALIPSO mission: spaceborne lidar for observation of aerosols and clouds. Proc. Spie, vol. 4893, 11 pp.